The Henryk Niewodniczański
INSTITUTE OF NUCLEAR PHYSICS
Polish Academy of Sciences
152 Radzikowskiego str., 31-342 Kraków, Poland

www.ifj.edu.pl/reports/2005.html

Kraków, January 2005

REPORT No 1957/PN

Measurements of the effective thermal neutron absorption cross-section in multi-grain models

Krzysztof Drozdowicz, Barbara Gabańska, Andrzej Igielski,
Ewa Krynicka, Krystyna Schneider, Urszula Woźnicka

Abstract

The effective macroscopic absorption cross-section Σ_a^{eff} of thermal neutrons in a grained medium differs from the corresponding cross-section Σ_a^{hom} in the homogeneous medium consisting of the same components, contributing in the same amounts. The ratio of these cross-sections defines the grain parameter, G, which is a measure of heterogeneity of the system for neutron absorption. Heterogeneous models have been built as two- or three-component systems (Ag, Cu and Co_3O_4 grains distributed in a regular grid in Plexiglas, in various proportions between them). The effective absorption cross-section has been measured and the experimental grain parameter has been found for each model. The obtained values are in the interval $0.34 < G < 0.58$, while $G = 1$ means the homogeneous material.

1. Introduction

The thermal neutron macroscopic absorption cross-section Σ_a is one of main parameters of the thermal neutron diffusion process in a medium. For a homogeneous mixture the Σ_a value can be obtained from the simple relation (based on Beckurts, 1964):

$$\Sigma_a = \rho \sum_i q_i \Sigma_{ai}^M , \tag{1}$$

where ρ is the mass density of the mixture, q_i is the mass contribution ($\sum q_i = 1$), and Σ_{ai}^M is the mass absorption cross-section of the i-th component (dependent on its elemental composition and on the microscopic absorption cross-sections σ_j of the contributing elements). Sometimes, it is convenient to express the contributions by the volume contents of components:

$$\phi_i = \frac{V_i}{V} , \tag{2}$$

where V_i is the volume occupied by the i-th component in the total volume V of the sample. Then Eq. (1), still for the homogeneous mixture, yields:

$$\Sigma_a = \Sigma_a^{hom} = \sum_i \phi_i \Sigma_{ai} , \tag{3}$$

where Σ_{ai} is the linear macroscopic absorption cross-section of the i-th component (Σ_{ai} are the values at the solid material density of the components).

For a heterogeneous mixture (strongly absorbing grains embedded in a low absorbing matrix) the measured absorption cross-section can significantly differ from that of the homogeneous one consisting of the same components in the same proportions. A simplified theoretical formula for the effective absorption cross-section for the two-component grained mixture was obtained by Drozdowicz *et al.* (2001a) and experimentally verified on well-defined dedicated models (Drozdowicz *et al*., 2001b). Later the approach was applied for geological materials (Woźnicka *et al*., 2003) in which grains are spread irregularly. A comprehensive description and a few applications are summarized in the paper by Drozdowicz *et al.* (2003). A theoretical solution for the calculation of the effective absorption cross-section for materials containing a few different types of absorbing centers is being developed (Schneider, 2004), based on the same physical approach as used in considerations by Drozdowicz *et al*. (2001a).

The effective thermal neutron absorption cross-section Σ_a^{eff} of the heterogeneous

mixtures can be obtained from a relation like in Eq. (3) but the cross-sections of individual components should include an influence of the heterogeneity effect.

Generally, the effective absorption cross-section $\Sigma_{\mathrm{a}}^{\mathrm{eff}}$ of the grained mixture can be estimated from the relation:

$$\Sigma_{\mathrm{a}}^{\mathrm{eff}} = \sum_i \phi_i \widetilde{\Sigma}_{\mathrm{a}i} \,, \tag{4}$$

where

$$\widetilde{\Sigma}_{\mathrm{a}i} = \frac{\Sigma_{\mathrm{a}i}}{\bar{d}_i \Sigma_{\mathrm{d}i}} \tag{5}$$

is the effective absorption cross-section for the grain which has the average size defined by the average chord length $\bar{d}_i = \dfrac{4V_{\mathrm{gr}\,i}}{S_{\mathrm{gr}\,i}}$ (Sjöstrand, 2002). $V_{\mathrm{gr}i}$ and $S_{\mathrm{gr}i}$ are the volume and surface of the grain, and $\Sigma_{\mathrm{d}i}$ is the diffusion cross-section of the i-th material:

$$\Sigma_{\mathrm{d}i} = \Sigma_{\mathrm{a}i} + (1 - \mu_i)\, \Sigma_{\mathrm{s}i} = \Sigma_{\mathrm{a}i} + \Sigma_{\mathrm{tr}i} \tag{6}$$

where Σ_{s} is the scattering cross-section and μ is the average cosine of the scattering angle. We define also the dimensionless size of the grain:

$$Y_i = \bar{d}_i \Sigma_{\mathrm{d}i} \tag{7}$$

which is the average size of the grain expressed in the neutron diffusion mean free paths.

The grain parameter is defined as the ratio:

$$G = \frac{\Sigma_{\mathrm{a}}^{\mathrm{eff}}}{\Sigma_{\mathrm{a}}^{\mathrm{hom}}}, \tag{8}$$

which is a function of the dimensionless grain sizes Y_i, of the ratios of the cross-sections of grain materials to the material of the matrix (i = 1): $S_i = \Sigma_{\mathrm{a}i}/\Sigma_{\mathrm{a}1}$, and of the volume contributions ϕ_i of the materials (Drozdowicz *et al.*, 2001a).

In the present report, results of series of measurements of the effective absorption cross-sections of different heterogeneous mixtures are presented. The models, which have been used in the measurements, contain simultaneously various types of grains, always in the same geometrical grid and in the same geometrical dimensions.

2. Measurement method and the materials used

The Czubek's pulsed method has been used to measure the macroscopic absorption cross-section Σ_a^{eff} of heterogeneous materials. The principles of Czubek's measurement method are summarized in the paper by Czubek *et al.* (1996). The experimental set-up consists of the investigated cylindrical sample of the fixed size ($H_1 = 2R_1$), surrounded by a cylindrical moderator ($H_{2g} = 2R_{2g}$) covered with a cadmium shield. The measurement geometry is shown in Fig. 1.

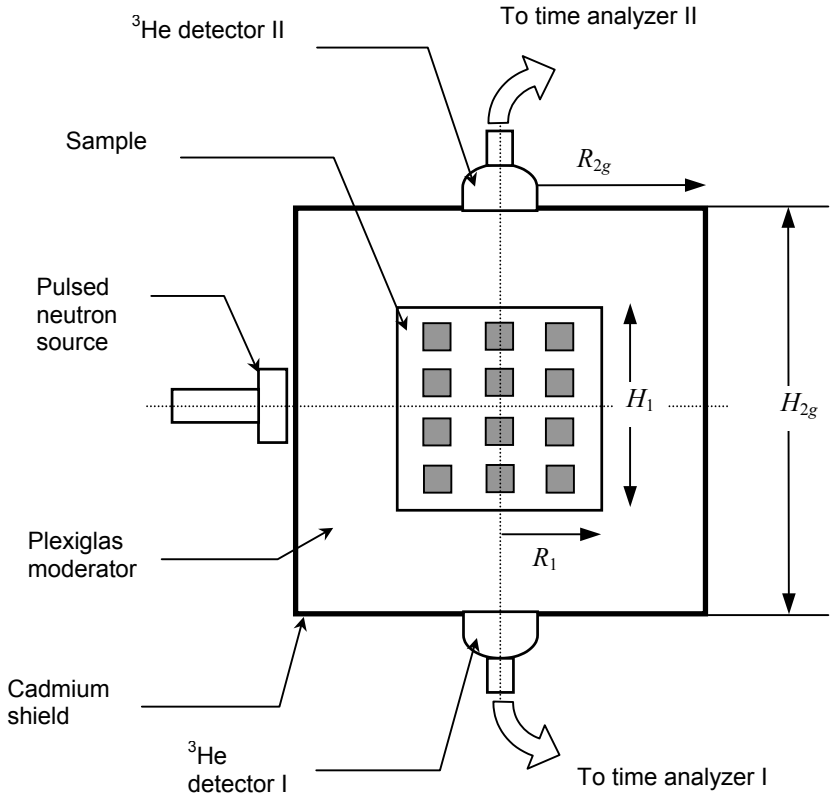

Fig.1. Experimental set-up (Drozdowicz *et al.*, 2003).

The system is irradiated by bursts of 14 MeV neutrons. Neutrons slow down in the system and form the thermal neutron field decaying in time. The fundamental exponential mode of the time decay constant λ_0 is the result of the measurement. The experiment is repeated using different sizes H_{2g} of the outer moderator. The experimental dependence $\lambda_0=\lambda_0(1/H_{2g}^2)$ is obtained. The curve $\lambda_0(1/H_{2g}^2)$ together with a certain theoretical solution for the thermal neutron flux in such two–medium system, $\lambda_0^*=\lambda_0^*(1/H_{2g}^2)$, allows to determine the

absorption rate $v\Sigma_{a1}$ of the material of the inner cylinder. The thermal neutron diffusion parameters of the outer medium (the absorption rate $v\Sigma_{a2}$, the diffusion constant D_{02} and the diffusion cooling coefficient C_2) and the geometrical dimensions of the system have to be known for calculations of this theoretical function λ_0^*. The $v\Sigma_{a2}$ and D_{02} values are given as for the infinite homogeneous material (here Plexiglas, Table 1). The parameter C_2 used in the calculation for this two-region system differs from the diffusion cooling coefficient known for the homogeneous medium (Krynicka *et al.*, 2001). It depends on the thermal neutron scattering properties of the materials and on the external moderator thickness. Finally it can be expressed as a function of the theoretical decay constant being just calculated, $C_2^* = C_2^*(\lambda_0^*)$. It is used in the interpretation in the Czubek's measurement method.

Table 1. Properties of the outer moderator shell of Plexiglas, $(C_5H_8O_2)_n$, at 20°C.

R_1	H_1	$H_{2g} = 2R_{2g}$	ρ	$v\Sigma_{a2}$	D_{02}	C_2
[cm]	[cm]		[g cm^{-3}]	[s^{-1}]	[cm^2 s^{-1}]	[cm^{4}s^{-1}]
4.5	9.0	variable	1.176	4 169	36 542	function $C_2^*(\lambda^*)$

The idea, how to cut properly a finite sample from an infinite grid of grains in the matrix material, was shown in the paper by Drozdowicz *et al.* (2001b). Three different sizes of silver grains were used in those experiments, resulting in three different effective macroscopic absorption cross-sections. In the present experiments, the effective absorption is measured when only one size of grains is used but they are composed of materials characterized with different thermal neutron absorption.

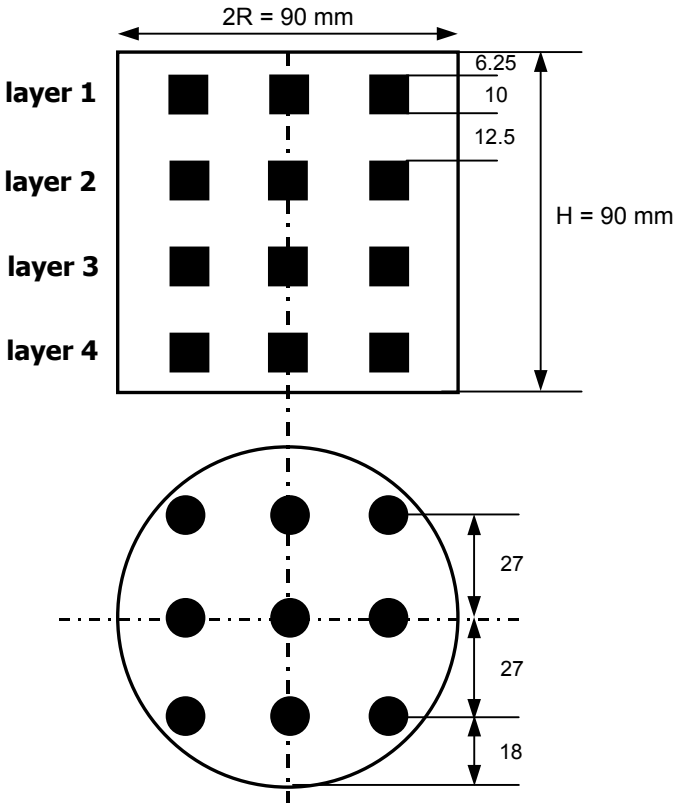

Fig.2. Structure of the cylindrical sample with the small cylindrical grains.

The small cylindrical grains are coaxial with the entire cylindrical model. The vertical and horizontal sections of the model are shown in Fig. 2. The height of the grains is $H_{gr} = 1$ cm and is equal of its diameter. The model contains 36 grains, which establish ~5 % of the sample volume. Thermal neutron diffusion parameters of the materials used for the construction of the grains are given in Table 2 (including an influence of the trace elements given in Appendix). The realized combinations are defined in Table 3.

Table 2. Thermal neutron diffusion parameters (v_0 = 2200 m/s) of the materials used for the construction of the grains.

Material	$\Sigma_a(v_0)$	$\Sigma_s(v_0)$	$\Sigma_d(v_0)$	ρ
	[cm^{-1}]	[cm^{-1}]	[cm^{-1}]	[g cm^{-3}]
Silver, Ag	3.71 ± 0.02	0.298 ± 0.001	4.01 ± 0.03	10.5
Copper, Cu	0.315 ± 0.002	0.642 ± 0.002	0.946 ± 0.004	8.70
Cobalt(II,III)oxide, Co_3O_4	1.54 ± 0.02	0.449 ± 0.002	1.98 ± 0.02	5.43

Table 3. Two- and three-component heterogeneous systems used in the Σ_a^{eff} measurements.

Two-component system		Three-component system	
Code	Contents	Code	Contents
PLX+Ag(n_1)	Plexiglas + n_1 silver grains	PLX+Ag(n_2)+Cu(n_3)	Plexiglas + n_2 silver grains + n_3 copper grains
PLX+Co_3O_4(n_4)	Plexiglas + n_4 cobalt oxide grains	PLX+Ag(n_5) +Co_3O_4(n_6)	Plexiglas + n_5 silver grains + n_6 cobalt oxide grains

The cylindrical grains of silver and copper have been made of rods of 1 cm in diameter. High-purity materials have been used (0.9999 Ag or 0.999 Cu, respectively). Elemental composition of the copper rods (M1E) is given in the Appendix (Table A1).

The cylindrical grains of cobalt oxide have been made of the powdered material using the method of hot-pressing. In this method the Co_3O_4 powder was parched in the special device with demand diameter under the high temperature and the high pressure. The sizes of grains are constant: $H_{gr} = 2R_{gr} = 1$ cm. The mass densities of individual grains differ slightly which is shown in Fig. 3. For the experiments, 36 cobalt oxide grains have been chosen for which the densities are closest to the maximum of the Gaussian curve. The mean density of these grains is 5.43 ± 0.09 g cm^{-3}. Two other cobalt oxide grains were checked against a

presence of impurities. The results are given in the Appendix in Table A2.

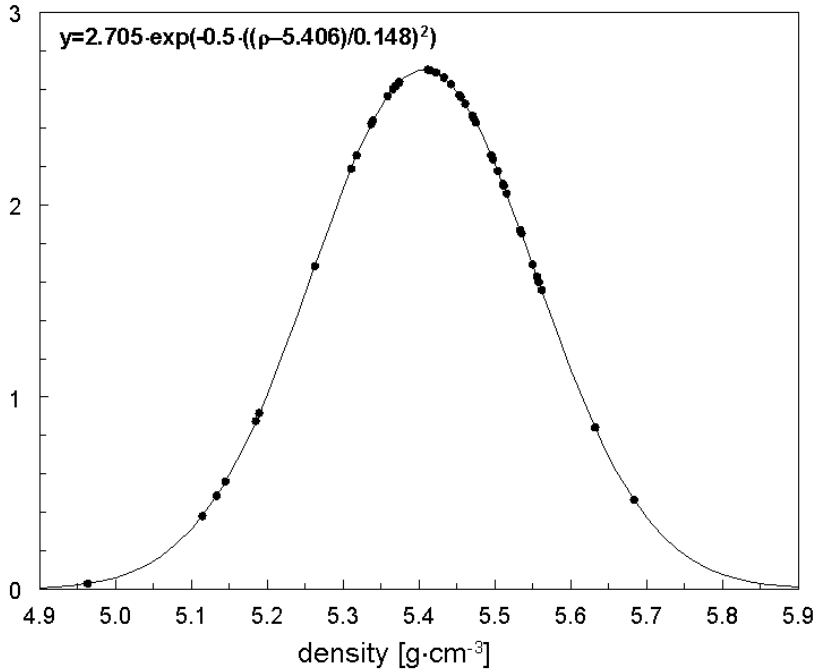

Fig.3. Distribution of the mass density of the Co_3O_4 grains.

3. Experimental results

All experiments have been performed in the desribed above two-region cylindrical geometry at the temperature of 20 ± 0.1 °C.

3.1. Two-component model [PLX+Ag(36)]

The experiment for the two–component system with silver grains has been repeated to engage the former experiments (Drozdowicz *et al.*, 2001b) with the present series. The distribution of the silver grains in the sample is presented in Fig.2. The time decay constants λ_0 measured in the present series are listed in Table 4. They are the mean values obtained from the time distributions recorded by the multiscalers attached to the top and the bottom ^{3}He detectors (Fig.1). The symbol $\sigma(x)$ marks one standard deviation of the x value. The obtained absorption rate $v\Sigma_{a1}$ and the effective absorption cross-section Σ_a^{eff} of the [PLX+Ag(36)] heterogeneous system are presented in Table 5. The conformity of the results of both series is excellent, which permits us to discuss later all results together.

Table 4. Results of the λ_0 measurements for the [PLX+Ag(36)] system.

H_{2g} [cm]	λ_0 [s^{-1}] $\sigma(\lambda_0)$ [s^{-1}]
14.0	16 732 57
	16 761 62
14.4	15 803 53
	15 956 87
14.8	15 157 78
	15 238 30
15.2	14 513 75
	14 517 74
16.0	13 355 67
	13 287 52

Table 5. Effective absorption cross-section of the [PLX+Ag(36)] system.

Series	$\nu\Sigma_{a1}$ $\sigma(\nu\Sigma_{a1})$	$\Sigma_a^{eff}(v_0)$ $\sigma[\Sigma_a^{eff}(v_0)]$	Experiment Code
	[s^{-1}]	[cm^{-1}]	
Present	15 022 64	0.0683 0.0004	GR10A
Elder [a)]	14 999 59	0.0682 0.0004	GR10

[a)] Drozdowicz *et al*. (2003)

3.2. Two-component model [PLX+Co_3O_4(36)]

The new two-component system has been built using cobalt oxide as the grain absorbers. The distribution of the grains in Plexiglas matrix is the same as in the case of the [PLX+Ag(36)] model (Fig. 2.). The absorption cross-section of cobalt oxide is lower than of the silver. The experiment allows showing the dependence of the grain parameter *G* on the absorption cross-sections of the grains. The measured time decay constants are collected in Table 6. The interpreted absorption rate $\nu\Sigma_{a1}$ and the Σ_a^{eff} values are given in Table 7.

Table 6. Results of the λ_0 measurements for the [PLX+Co_3O_4(36)] system.

H_{2g} [cm]	λ_0 [s^{-1}] $\sigma(\lambda_0)$[s^{-1}]
14.8	13 864 33
	13 840 27
15.2	13 292 28
	13 320 43
16.0	12 369 28
	12 312 83
17.0	11 180 37
	11 188 43

Table 7. Effective absorption cross-section of the [PLX+Co_3O_4(36)] system.

$\nu\Sigma_{a1}$ $\sigma(\nu\Sigma_{a1})$	$\Sigma_a^{eff}(v_0)$ $\sigma[\Sigma_a^{eff}(v_0)]$	Experiment Code
[s^{-1}]	[cm^{-1}]	
12 005 87	0.0546 0.0004	Co10A

3.3. Three-component model [PLX+Ag(30)+Cu(6)]

The three-component system of the same total volume content of absorbers (4.94 %) as in the two-component arrangement (Drozdowicz *et al.*, 2001b) has been built. The model contains 30 silver (about 4.12 %) and 6 copper (about 0.82 %) grains in the Plexiglas (95.06 %) matrix. The difference between the neutron diffusion parameters of silver and copper (Table 2) should cause that the effective absorption cross-section of the three-component heterogeneous system differs from the Σ_a^{eff} value of the two-component [PLX+Ag(36)] system.

Fig. 4 presents distributions of the silver and copper grains in the sample. Three variants of the disposition of the grains in the sample have been investigated:

Variant (i): copper grains are situated in interior layers of the sample,

Variant (ii): copper grains are situated in exterior layers of the sample,

Variant (iii): copper grains are located in the first and third layer of the sample (or symmetrically, *i.e.* in the 2nd and 4th layer).

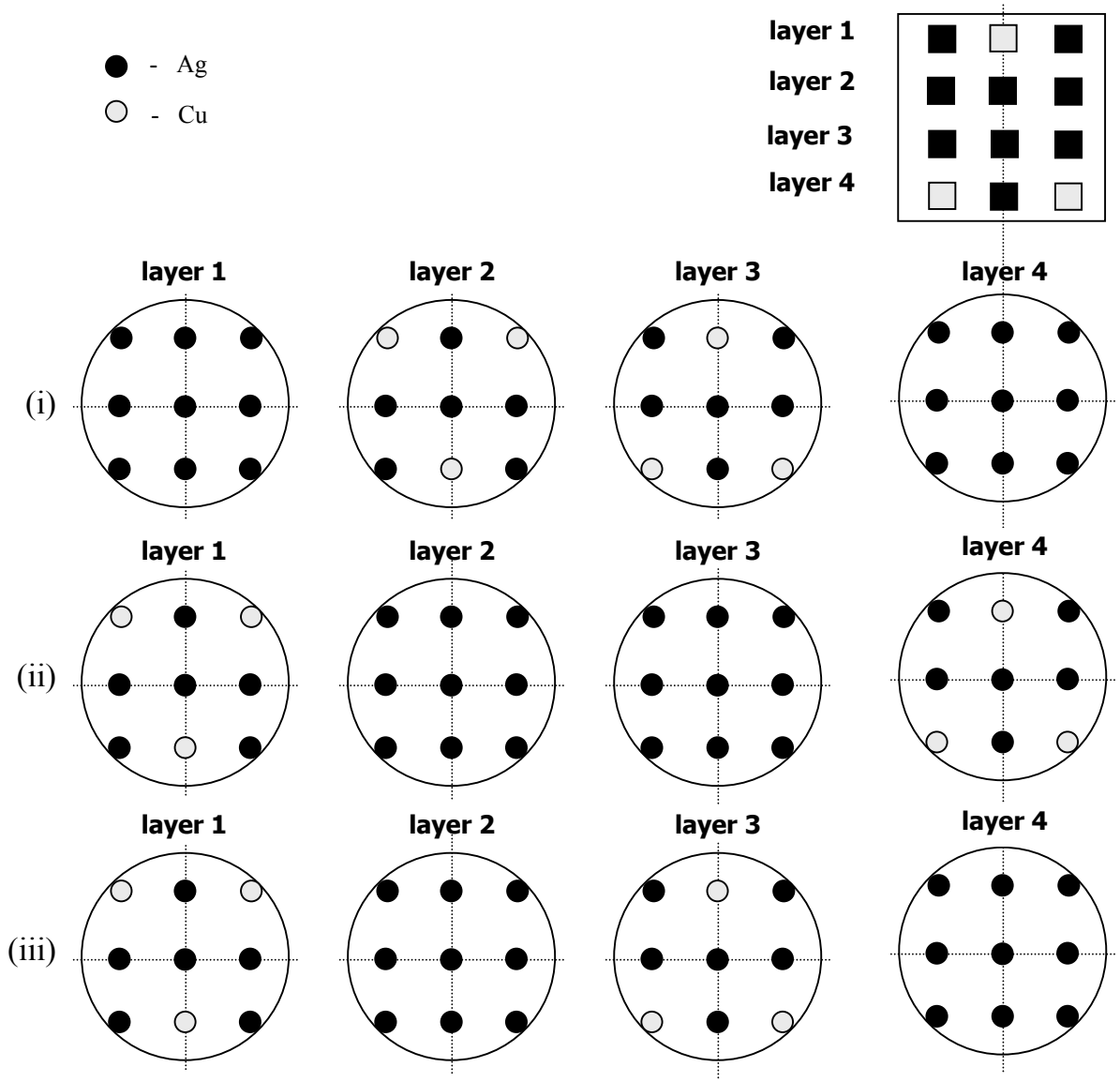

Fig.4. Distribution of silver and copper grains in the three-component system [PLX+Ag(30)+Cu(6)].

The effective absorption cross-sections have been measured for the all variants to detect a possible effect of the grain distribution in the Plexiglas matrix on the result. The decay constants λ_0, measured for the all variants of the [PLX+Ag(30)+Cu(6)] arrangements, are presented in Table 8.

The obtained effective absorption cross-sections of the [PLX+Ag(30)+Cu(6)] system in the three variants are given in Table 9. There are also shown the absolute $\Delta\Sigma_a^{eff}$ and relative $\Delta\Sigma_a^{eff}/\Sigma_a^{eff}(i)$ differences of the results in comparison to Variant (i).

Table 8. Results of the λ_0 measurements for three variants of the [PLX+Ag(30)+Cu(6)] system.

H_{2g}	Variant (i)		Variant (ii)		Variant (iii)	
	λ_0	$\sigma(\lambda_0)$	λ_0	$\sigma(\lambda_0)$	λ_0	$\sigma(\lambda_0)$
[cm]	[s^{-1}]	[s^{-1}]	[s^{-1}]	[s^{-1}]	[s^{-1}]	[s^{-1}]
14.8	14 603	75	14 531	73	14 593	58
	14 602	65	14 520	67	14 680	50
					14 627	69
					14 639	107
15.2	13 987	54	13 961	47	14 021	58
			13 966	52	14 026	54
					14 037	50
					14 016	62
16.0	12 905	47	12 725	76	12 881	60
	12 840	52	12 766	54	12 870	73
					12 906	72
					12 904	77
17.0	11 640	54	11 585	40	11 617	66
	11 618	55	11 564	52	11 637	38
					11 655	61
					11 660	52

Table 9. The effective absorption cross-sections for all variants of the [PLX+Ag(30)+Cu(6)] system.

Variant	$\nu\Sigma_{a1}$ $\sigma(\nu\Sigma_{a1})$	$\Sigma_a^{eff}(v_0)$ $\sigma[\Sigma_a^{eff}(v_0)]$	$\Delta\Sigma_a^{eff}$	$\frac{\Delta\Sigma_a^{eff}}{\Sigma_a^{eff}(i)}$	Experiment Code
	[s^{-1}]	[cm^{-1}]	[cm^{-1}]		
(i)	13 596 71	0.0618 0.0003	0	0	CuAg10
(ii)	13 394 72	0.0609 0.0003	–0.0009	–0.015	CuAg10A
(iii)	13 644 65	0.0620 0.0004	0.0002	0.003	CuAg10B

3.4. Three-component model [PLX+Ag(30)+Co_3O_4(6)]

The model [PLX+Ag(30)+Co_3O_4(6)] is analogous to the model described in paragraph 3.3. The cobalt oxide grains are used in place of the copper grains. Thus, the volume contents are still the same as previously: Plexiglas 95.06 %, silver ~4.12 %, and Co_3O_4 ~0.82 %. Variants (i) and (ii) of the grain distribution are the same as in the case [PLX+Ag(30)+Cu(6)].

The next structure is different:

Variant (iv): the cobalt oxide grains are placed in the each layer, as shown in Fig. 5.

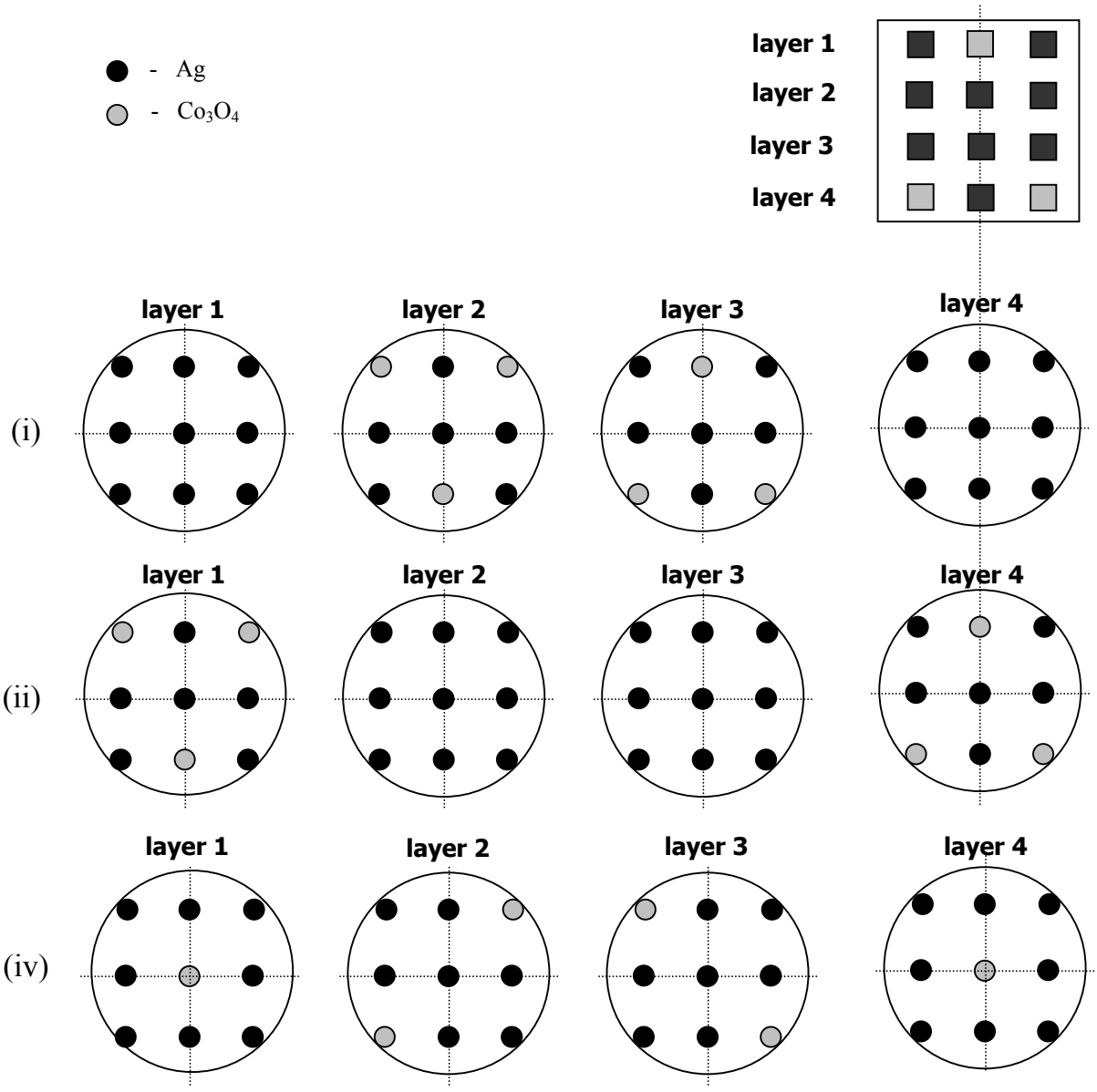

Fig.5. Distribution of the silver and cobalt(II,III)oxide grains in the three-component system [PLX+Ag(30)+Co_3O_4(6)].

The results of the λ_0 measurements for the all variants of the [PLX+Ag(30)+Co_3O_4(6)] arrangements are presented in Table 10.

The effective absorption cross-sections for the three variants of the grain distributions are presented in Table 11. The differences between the obtained results are insignificant.

Table 10. Results of the λ_0 measurements for three variants of the [PLX+Ag(30)+Co_3O_4(6)] system.

H_{2g}	Variant (i)		Variant (ii)		Variant (iv)	
	λ_0	$\sigma(\lambda_0)$	λ_0	$\sigma(\lambda_0)$	λ_0	$\sigma(\lambda_0)$
[cm]	[s^{-1}]	[s^{-1}]	[s^{-1}]	[s^{-1}]	[s^{-1}]	[s^{-1}]
14.0	16 541	60				
	16 510	81				
14.4	15 695	33	15 709	49	15 702	44
	15 725	85	15 639	98	15 709	42
14.8	15 039	63	14 988	70	14 981	66
	15 029	42	15 004	65	14 968	56
15.2	14 296	41	14 380	62	14 353	71
	14 387	54	14 301	81	14 314	53
16.0	13 176	73	13 193	51	13 158	40
	13 169	29	13 066	40	13 141	30

Table 11. Effective absorption cross-sections in three variants of the [PLX+Ag(30)+Co_3O_4(6)] structure.

Variant	$\nu\Sigma_{a1}$ $\sigma(\nu\Sigma_{a1})$	$\Sigma_a^{eff}(v_0)$ $\sigma[\Sigma_a^{eff}(v_0)]$	Experiment Code
	[s^{-1}]	[cm^{-1}]	
(i)	14 541 69	0.0661 0.0003	CoAg10X
(ii)	14 473 69	0.0658 0.0003	CoAg10Y
(iv)	14 488 56	0.0659 0.0003	CoAg10W

3.5. Three-component model [PLX+Ag(18)+Co_3O_4(18)]

The three-component model with the equal volume content of the silver and cobalt oxide grains has been constructed, *i.e.*: Plexiglas 95.06 %, Co_3O_4 ~2.47 %, and silver ~2.47%. The distribution of the grains in presented in Fig. 6. The effective neutron absorption cross-section of the [PLX+Ag(18)+Co_3O_4(18)] system is lower than in the previous case [PLX+ Ag(30)+Co_3O_4(6)], because the absorption cross-section of cobalt oxide is lower than of silver. In the consequence the effect of granulation should be weaker. The results of the λ_0

measurements for the [PLX+Ag(18)+Co_3O_4(18)] arrangement are presented in Table 12.

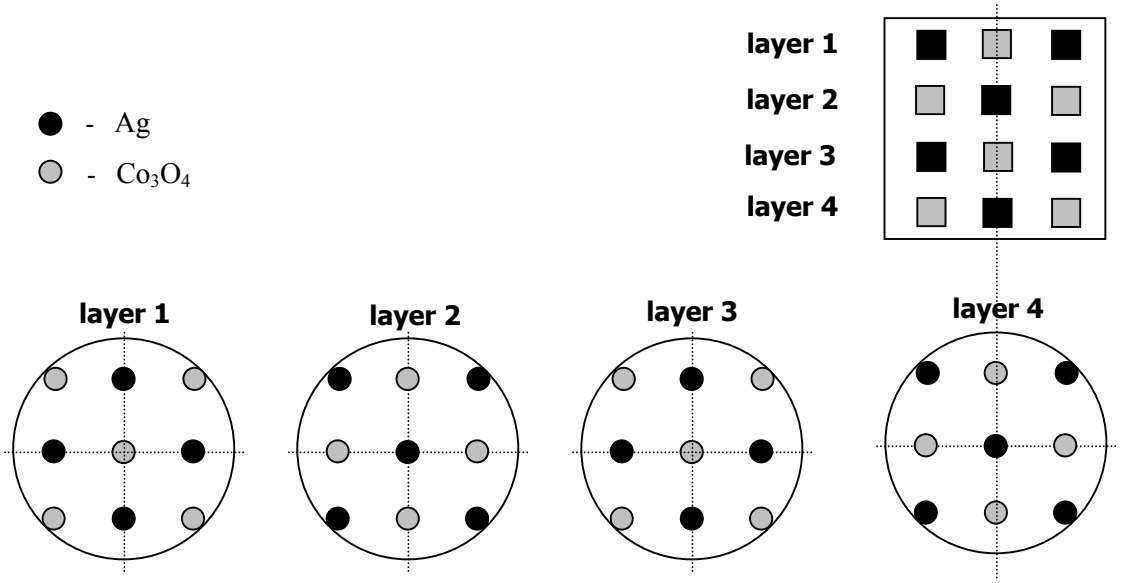

Fig.6. Distribution of the silver and cobalt(II,III)oxide grains in the three-component system [PLX+Ag(18)+Co_3O_4(18)].

Table 12. Results of the λ_0 measurements for the [PLX+Ag(18)+Co_3O_4(18)] system.

H_{2g} [cm]	λ_0 [s^{-1}] $\sigma(\lambda_0)$ [s^{-1}]
14.8	14 589 51
	14 493 84
15.2	13 912 77
	14 000 40
16.0	12 844 62
	12 816 59
17.0	11 623 67
	11 619 57

Table 13. Effective absorption cross-section of the [PLX+Ag(18)+Co_3O_4(18)] system.

$\nu\Sigma_{a1}$ $\sigma(\nu\Sigma_{a1})$	$\Sigma_a^{eff}(v_0)$ $\sigma[\Sigma_a^{eff}(v_0)]$	Experiment Code
[s^{-1}]	[cm^{-1}]	
13 500 70	0.0614 0.0003	CoAg10Z

4. Calculation of the grain parameters

The macroscopic absorption cross-sections $\Sigma_a = \Sigma_a^{hom}$ of the ideal homogeneous mixtures of components, corresponding to the considered heterogeneous systems, have been calculated from Eq. (3) using the neutron material parameters given in Tables 1 and 2. The grain parameter *G* has been calculated for each examined system from Eq. (8) using the experimental Σ_a^{eff} data. The results are presented in Table 14.

Table 14. Thermal neutron macroscopic absorption cross-sections Σ_a^{hom} for the homogeneous equivalents of the heterogeneous systems and the grain parameters *G* for two- and three-component systems.

Heterogeneous model	ϕ(Ag)	ϕ(Cu)	ϕ(Co_3O_4)	Σ_a^{hom} $\sigma(\Sigma_a^{hom})$ [cm^{-1}]	*G* σ(*G*)	Variant of the grain distribution
Two-component systems						
PLX+Ag(36)	0.04938	0	0	0.2013 0.0012	0.339 0.004	–
PLX+Co_3O_4(36)	0	0	0.04938	0.0941 0.0005	0.580 0.007	–
Three-component systems						
PLX+Ag(30)+Cu(6)	0.04115	0.00823	0	0.1733 0.0010	0.357 0.004	(i)
					0.351 0.004	(ii)
					0.358 0.004	(iii)
PLX+Ag(30)+Co_3O_4(6)	0.04115	0	0.00823	0.1834 0.0010	0.360 0.004	(i)
					0.359 0.004	(ii)
					0.359 0.004	(iv)
PLX+Ag(18)+Co_3O_4(18)	0.02469	0	0.02469	0.1477 0.0007	0.416 0.004	–

The grain parameter *G* depends on neutronic and geometrical parameters. The parameters, *S*, *Y*, and ϕ, calculated for the investigated models are collected in Table 15.

Table 15. Neutronic and geometrical parameters of the components used in the investigated heterogeneous systems.

Material i	$S_i = \Sigma_{ai}/\Sigma_{aPlexi}$ $\sigma(S_i)$	Y_i $\sigma(Y_i)$ [mfp]	ϕ
$(C_5H_8O_2)_n$	1	4.6 0.2	0.9506
Ag	195.3 1.7	2.67 0.02	total 0.0494
Cu	16.6 0.1	0.631 0.003	
Co_3O_4	81.1 0.3	1.29 0.03	

5. Conclusions

The dedicated heterogeneous models used in the experiments are characterized with the constant geometrical size of the grains placed in the Plexiglas matrix in a constant geometrical grid. The volume content of the Plexiglas is always ~95 %, the remaining volume is occupied by one or two types of the absorbing grains. The ratio of the absorption cross-sections S_i and the dimensionless size Y_i are the variable parameters. Unfortunately, it is impossible to observe in a real experiment the variability of the grain parameter, G, as a function of only one parameter, S_i or Y_i, while the second parameter is fixed. The S parameter is expressed by the absorption cross-sections and Y depends both on the absorption, Σ_a, and scattering, Σ_s, cross-sections. It is rather impossible to built the grains of different materials which are characterized with exactly the same Σ_a cross-section and different Σ_s cross-sections, or *vice versa*, in order to investigate experimentally an isolated function of one variable, for example $G= G(\Sigma_a)$. However, it is always possible to define the experimental G value, *i.e.* to determine the ratio of the measured effective absorption cross-section to the cross-section of the corresponding homogeneous material.

The grain parameter $G = 1$ means the homogeneous medium from the point of view of the thermal neutron absorption during the transport. The G value always decreases with an increase of heterogeneity of the system.

A very high heterogeneity effect, $G \approx 0.34$, has been observed for the two-component system, [PLX+Ag(36)]. That system is characterized by the highest S_i and Y_i values among the models prepared. The absorption has been later decreased by replacement of six Ag grains

with the Co_3O_4 or Cu grains. The Σ_a^{hom} cross-section is then respectively 8.9 % or 13.9 % lower than for the [PLX+Ag(36)] model. This change has had a very weak influence on the change of the *G* parameter ($G \approx 0.36$). This example shows how complex the dependence of the *G* parameter on the material properties is (although the geometrical size of the grains is constant). The small differences between the obtained *G* values are caused by a simultaneous significant change of the Y_i size, relative to the changed neutron mean free path (Table 15).

The highest difference between the *G* parameters is observed between the [PLX+Ag(36)] and [PLX+Co_3O_4(36)] models: $G \approx 0.34$ and 0.58, respectively. In this two cases the Σ_a^{hom} cross-section changes 2.1 times, and the measured grain parameter, *G*, changes 1.7 times. This non-proportional change is again caused by a change of the Σ_s cross-section, *i.e.* the change of the grain size *Y* "seen" by neutrons.

The presented experimental results can be interpreted using a theoretical approach to the effective absorption of thermal neutrons in materials which contain more than one type of strongly absorbing grains. The theory is just being developed (Schneider, 2004).

As shown, it would be very difficult (or almost impossible) to prepare more samples in which only one of the neutron material parameter would be variable. Instead, a continuation of the research can be completed with numerical simulations of such experiments, provided that the conformity between the real experiments and their simulations is achieved.

References

Beckurts K.H., Wirtz K. (1964)
Neutron Physics.
Springer, Berlin.

Czubek J.A., Drozdowicz K., Gabańska B., Igielski A., Krynicka E., Woźnicka U. (1996)
Thermal neutron macroscopic absorption cross section measurement applied for geophysics.
Progr. Nucl. Energy **30**, 295-303.

Drozdowicz K. Gabańska B., Igielski A., Krynicka E., Woźnicka U. (2003)
The effective absorption cross-section of thermal neutrons in a medium containing strongly or weakly absorbing centres.
Cent. Eur. J. of Phys. **2**, 210-234.

Drozdowicz K., Gabańska B., Krynicka E., Woźnicka U. (2001a)
Influence of the grain size on the effective absorption cross-section of thermal neutrons in a medium containing highly absorbing centres.
Ann. Nucl. Energy **28**, 1485-1497.

Drozdowicz K., Gabańska B., Igielski A., Krynicka E., Woźnicka U. (2001b)
A pulsed measurement of the effective thermal neutron absorption cross-section of a heterogeneous medium.
Ann. of Nucl. En. **28**, 519-530.

Krynicka E., Gabańska B., Woźnicka U., Dąbrowska J., Burda J. (2001)
Interpretation problems of Czubek's Σ_a measurement method. Reference experiment on H_3BO_3 solutions.
Report INP No 1890/PN. IFJ PAN, Kraków. http://www.ifj.edu.pl/reports/1890.pdf

Schneider K. (2004)
Influence of the granulation parameters of the heterogeneous system on the thermal neutrons absorption. PhD thesis.
Institute of Nuclear Physics Polish Academy of Sciences, Kraków (in Polish).

Sjöstrand N.G. (2002)
What is the average chord length?
Ann. Nucl. Energy **29**, 1607-1608.

Woźnicka U., Drozdowicz K., Gabańska B., Krynicka E., Igielski A. (2003)
Are geological media homogeneous or heterogeneous for neutron investigations?
Appl. Radiat. Isot. **58**, 131-136.

XRAL (2004)
XRAL Laboratories: Geochemical Exploration and Research Analysis, Canada.

Appendix. Material specifications.

Copper grains

Table A1. Elemental composition of the M1E rods

Component	[%]
Cu	**99.9**
Bi	0.001
Pb	0.005
Sb	0.002
As	0.002
Fe	0.005
Ni	0.002
Zn	0.005
S	0.005
O_2	0.06
Ag	0.003

The bulk density of the grains is

$$\rho_B = \frac{m_g}{V_g} = 8.703 \pm 0.001 \text{ g cm}^{-3}.$$

The solid material density measured in a helium pycnometer is $\rho_P = 8.926 \pm 0.004$ g cm^{-3}.

Cobalt(II,III)oxide grains

Table A2. Trace element content in the Co_3O_4 grains (XRAL, 2004)

Component	[ppm]
Co_3O_4	**999 966**
Gd	0.06 ± 0.05
Sm	0.1 ± 0.1
Eu	< 0.05
Th	3.9 ± 0.1
U	< 0.05
Zr	19.4 ± 0.5
B	<10

The average bulk density of the Co_3O_4 grains $\rho_B = 5.43 \pm 0.09$ g cm^{-3} has been found as described at the end of paragraph 2. The details are presented by Schneider (2004).

The density from the helium pycnometer is $\rho_P = 6.055 \pm 0.006$ g cm^{-3} and the solid matherial density reported by the producer is $\rho_S = 6.110$ g cm^{-3}. This defines the porosity of the constructed grains to 11 %.

Material composition of the investigated models

Table A3. Mass and volume relations of components in particular experimental models.

Model		PLX+ Ag(36)	PLX+ Co_3O_4(36)	PLX+Ag(30) +Cu(6)	PLX+Ag(30) +Co_3O_4(6)	PLX+Ag(18) +Co_3O_4(18)
Ag	m [g]	296.877	-	247.398	247.398	148.439
	q [%]	31.685	-	26.645	27.095	17.155
	V [cm^3]	28.274	-	23.562	23.562	14.137
	ϕ [%]	4.938	-	4.115	4.115	2.469
Co_3O_4	m [g]	-	153.56	-	25.593	76.78
	q [%]	-	19.349	-	2.803	8.873
	V [cm^3]	-	28.274	-	4.712	14.137
	ϕ [%]	-	4.938	-	0.823	2.469
Cu	m [g]	-	-	41.013	-	-
	q [%]	-	-	4.417	-	-
	V [cm^3]	-	-	4.712	-	-
	ϕ [%]	-	-	0.823	-	-
PLX [a)]	q [%]	68.315	80.651	68.937	70.102	73.972
Total sample [b)]	m_1 [g]	936.951	793.634	928.485	913.065	865.293
	ρ_1 [g cm^{-3}]	1.636	1.386	1.622	1.595	1.511

[a)] PLX = Plexiglas, total mass is always m_{PLX} = 640.074 g, the volume contribution is ϕ_{PLX} = V_{PLX}/V_1 = 95.062 %.

[b)] Total volume of the sample is always V_1 = 572.555 cm^3.